Final Report: Measurement of firebrands generated during fires in pine-dominated ecosystems in relation to fire behavior and intensity

Table of Contents

List of Tables

List of Figures

List of Keywords

Firebrands, wildland urban interface, WUI, firebrand flux, firebrand deposition, fire line intensity, fire behaviour, firebrand generation.

List of Abbreviations

CDF, cumulative distribution function
CFD, computational fluid dynamics
FBP, fire behaviour package
FCS, firebrand collection site
PPS/N, Parker Preserve South/North
TT, tall timbers
WUI, wildland urban interface

Acknowledgements

We are grateful to JFSP for supporting this project. Many thanks to the NJ Forest Fire Service without whom the field experiments would not have been possible. Special thanks to Dr Michael Gallagher for huge efforts in coordinating and Dr Kenneth Clark for support during the field campaigns. Prof Albert Simeoni supported this work throughout and it would not have been possible without him.

Abstract

Firebrands are a leading cause of ignition at the wildland urban interface and a driver of rapid fire spread during wildfires. Current studies which seek to evaluate this risk are limited by a paucity of data relating to the firebrand dynamics from real fires. In particular the deposition of firebrands as a function of time and space relative to the fireline and the propensity for firebrands to result in ignition of structural materials.

This project sought to join these areas by accurately measuring the firebrand deposition from head fires and relating this to the fire behaviour. The primary objectives were to measure the fire behaviour, and firebrand deposition. This was complimented by an assessment of the risk posed by firebrands in structure ignitions and an implementation of firebrand generation and transport in a numerical model (Fire Dynamics Simulator).

Novel data collection techniques were developed to satisfy these objectives. Fire behaviour (spread and intensity) was measured using a network of bespoke, GPS enabled temperature loggers (FireTrackers) complimented by a lower density array of flame height measurements. Local wind velocity was also measured. Firebrand measurements were primarily made by collection in cans distributed downwind of the fire. Addition of video recording at the collection sites allowed the time dependence to be evaluated such that firebrand deposition dynamics could be linked to fire behaviours.

The key findings of the project are that: firebrand deposition dynamics are linearly proportional to increases in fire behaviour; firebrand deposition occurred up to 200 m from the fire line (for the fires and conditions studied); ignition of materials is dependent on the smouldering characteristics of firebrand accumulations.

The methodology as presented can be adopted during other prescribed or management fires to add to the data set and generate a set of consistent knowledge within the community. The data collected can be used when planning and evaluating the risk posed by management in similar systems and environmental conditions to those studied here. The data are also useful for development of methods aimed at reducing the firebrand ignition risk at the WUI and in ensuring the design of future experimental investigations is relatable to realistic conditions.

Objectives

The original study objectives were as follows:

1. Evaluate the fire source (fire intensity, rate of spread, flame geometry) and its environment, (wind and fuel conditions).
2. Quantify ember[1] [firebrand] mass flux in relation to a fire source and the environmental and fuel conditions.
3. Assess the potential for structural ignition via ember [firebrand] showers based on range of potential scenarios, guided by in-situ observations of the field experiments, using materials and geometric configurations representative of WUI structures.

---

[1] Throughout this report the term "firebrand" is used to describe any particle ejected from a fire. This

4. Enhance the capacity of WFDS to describe ember [firebrand] showers and their impact on structures at the WUI, using coupled laboratory measurements and in-situ observations of the field experiments.

Objectives 1-3 were met within the constraints of this project. Objective 4 was partially met although there remain significant challenges in the ability for numerical models to reproduce wildfire behaviours required to drive the generation and deposition of firebrands. Therefore, only a preliminary investigation was possible which identified key challenges for future direction to accurately reproduced firebrand fluxes using numerical simulations.

Relation to task statement
The project addressed task statement 15-01-*04 Fire ember production*. The questions to be addressed by this call and the method by which they are addressed are given below.

- *What is the rate of ember production from burning wildland and structural fuels in the WUI under a range of environmental conditions? Are ember production rates related to commonly used environmental indices, e.g., Keetch Byram Drought Index, Haines Index, or the Energy Release Component.*

This question was addressed by Objectives 1 and 2. A series of large scale field experiments were undertaken in the New Jersey Pine Barrens and at the Tall Timbers Research Station & Land Conservancy (Florida) to evaluate firebrand generation under a range of fire intensities and environmental conditions.

- *What is the characteristic size and shape of embers produced from burning wildland and structural fuels in the WUI under a range of environmental conditions?*

This was addressed in Objectives 1 and 2. The firebrands collected from the field experiments fires were counted and characterised.

- *How far can embers of characteristic size and shape travel under a range of wind speeds?*

This was addressed in Objectives 1 and 2. The firebrand deposition at different locations from the fire front was quantified in real time. Objective 4 identified the requirements of numerical modelling to evaluate this process.

- *How long can embers of characteristic size and shape burn and at what intensities?*

This was not addressed directly. Objective 3 identified the burning of firebrand accumulations and Objective 1 and 2, the condition of firebrands upon landing (through leveraged funding).

- *What is the role of ember production from wildland and structural fuels in fire spread in the WUI?*

Ignition of common structural fuels was evaluated in Objective 3.

Background

Introduction
Many studies have been conducted on the propensity of ignition of fuels by hot particles, single firebrands or simulated firebrand attack [1–8]. Nevertheless, there remains relatively little

information available on the characteristics of firebrands generated by wildfires. The primary characteristics that are required to describe the risk posed by firebrands are the mass flux and condition of the particles. In order to quantify these variables, measurements of the number, mass, shape, temperature, material properties and reaction condition of firebrands generated from fires are required. To provide appropriate context for these measurements, it is essential to relate the firebrands to measurements of the fuels present, the fire behaviour and the local meteorological conditions.

There are multiple characteristics that must be measured that define the hazard posed by firebrands. Extrinsic factors such as the fuels (vegetative or structural) that are present, the fire behaviour and the meteorological conditions will define the rate of generation of firebrands and the travel distance of the firebrands. Therefore, any firebrand measurements should include high temporal and spatial resolution measurements of these quantities.
The firebrand characteristics of shape and mass will determine the aerodynamic properties and hence the travel distance. The transport is further influenced the temperature evolution of the firebrand, including any potential combustion processes. The ignition potential of a firebrand is a combination of several factors including the characteristics of the firebrand upon landing, the energy content upon landing, the nature in which this energy is released and whether the problem relates to single firebrands or an accumulation of firebrands.
Consistent measurement of the firebrand fluxes from real fires is essential in order to understand the risks posed by firebrands e.g. spot fires or structure ignitions and to determine appropriate test methods to evaluate risk, assess mitigation strategies or to develop predictive tools.

Research background

Much of the work to date has focussed on understanding the ignition of structures at the WUI that may be subject to firebrand attack. Typically, studies simulate the ignition of structural materials such as wooden decking or roofing materials. In these scenarios, deposition typically occurs due to fluid mechanic considerations around obstruction in a flow. As a result, accumulations of firebrands form at stagnation points around a structure. An accumulation of firebrands may contain burning, hot or cold vegetative matter. If a hot or burning particle can cause ignition of this accumulation, then it is likely that the cold firebrands also deposited will burn. It is commonly observed that these accumulations burn as a smouldering fire. To adequately quantify the risk of these accumulations, the burning duration, energy available, area of impact and heat transfer to the substrate govern the ignition risk.

Firebrands also present a risk by accelerating or altering fire spread due to long and short range ‘spotting’. This process occurs when the firebrands are deposited on, and ignite natural fuels ahead of the fire line (these may be wildland fuels or ornamental vegetation). This mechanism has been observed at the short range in a number of experimental fires [9,10] and also over much longer distances in real wildfires [11,12]. In this case the ignition is determined by the travel distance of individual firebrands and ignition is (anecdotally) the result of a single firebrand. In this case the condition of the firebrand is key to assessing the ignition risk.

These two problems, although similar in nature, require somewhat different approaches to their study and hence different information is required to quantify the risk [1–4,8,13–17]. It is clear that the approach required to this problem will be statistical in nature and therefore efforts should be made to capture firebrands in quantities sufficient to lead to robust statistical analyses. This emphasises the need for a common understanding of the problem and common understanding of the experimental techniques necessary to consistently record this data.

Origin of firebrands

In the natural environment, firebrands may originate from bark fragments, branches, twigs and foliage and close to the Wildland Urban Interface (WUI) they may originate from structural materials [18]. The nature of the source material strongly dictates the characteristics of the firebrand.

The mechanisms that govern firebrand generation are not well understood, however, it appears that there are two predominant mechanisms, both of which require the mechanical separation of organic matter from a parent body. The first is the lofting of cold, organic matter which may or may not pass through the flame front. The second mechanism is the fracture of organic matter due to the loss of mechanical properties as it undergoes heating, pyrolysis and combustion [19]. There is competitively little study of the generation mechanisms from wildland fuels, however, species which are known to shed bark are logically assumed to produce a greater number of firebrands than a species which does not (assuming an equal fire exposure).

The second component of the origin of firebrands is understanding the dependence of firebrand generation of the fire environment. The fire environment generates the source term for the force (primarily due to buoyancy) to pick up and loft the firebrands. Therefore, in order to quantify and characterise the firebrands arising from a fire, it is necessary to understand the fuels present, the fire environment and the conditions for firebrand transport.
There has been very little work to identify the origin of firebrands from natural fuels. Methods presented by El Houssemi et al. [10] and Thomas et al. [20] form the basis for most ongoing experimental work. In experimental fires in the New Jersey Pine Barrens (*a Pinus rigida*, dominated system), the firebrand generation was measured by quantifying the change in diameter of a number of tree boles in the burn unit.

Transport of firebrands

The transport of firebrands is primarily an aerodynamics problem. There have been attempts made to predict the path or maximum transport distance of firebrands if the meteorological conditions are known. Nevertheless, these models generally suffer from uncertainty around the 'injection point' i.e. from where, and at what rate, particles are generated and injected into the plume. This uncertainty is fundamental to the challenge of quantifying firebrand risk. The burning of firebrands during transport has been investigated e.g. [21–25].

Deposition of firebrands

In measuring the deposition of firebrands, it is necessary to understand which aspects of the firebrands contribute to the risk. The following criteria will influence the ignition propensity of a firebrand or firebrand accumulation: number flux of firebrands, mass flux of firebrands, state of the firebrands (smouldering, flaming, hot, cold), the size, and size distribution, of firebrands, and the energy content of the firebrands upon landing. These parameters will vary as a function of distance from the fire line and will depend on the trajectory of the particle. The firebrand deposition must be quantified as a flux (mass, number or energy) relative to the position of the fire front.

Materials and Methods

Experimental quantification of firebrand generation and deposition
This section will discuss the techniques used to quantity firebrand generation and firebrand disposition. In order to allow interpretation of the results, fire behaviour must also be characterised and methods to do so are also briefly discussed. Measuring the generation of firebrands is essential to identify the efficacy of any collection technique.

The only approach at present to quantify firebrand generation and deposition is through large-scale experimentation primarily in the field. Due to the nature of these fires, detailed quantification of fire environment (e.g. meteorological conditions and fuels) is required, as well as high resolution measurements of fire behaviour (e.g. spread rate and heat release rate).

It has been shown that low intensity fires do not produce significant quantities of firebrands [20]. Thus, trying to quantify firebrand flux from operational prescribed burning, where the fire is usually a backing fire and may consist of multiple ignition lines is not desirable. Instead a head fire should be used.
This section will discuss the collection methods to obtain data to create:

- Firebrand size and mass characterization in the form of cumulative distribution functions.
- Total firebrand flux as a function of separation distance to burn unit for a given fire behaviour.
- Firebrand condition.
- Travel distances of firebrands.
- Total number and mass of firebrands deposited.

Quantification of the firebrand mass, energy content and char fraction must be undertaken on samples collected in field experiments.

Quantification of total firebrand number and mass flux
The firebrand flux needs to be resolved in spatial and temporal dimensions. A schematic of the spatial distribution of firebrands from a source is shown in Figure 1. Techniques for measuring firebrands involve capturing the firebrands upon landing. Thomas et al. [9] demonstrated the effectiveness using water-filled cans clustered in collection sites situated downwind of the fire in large-scale field experiments.

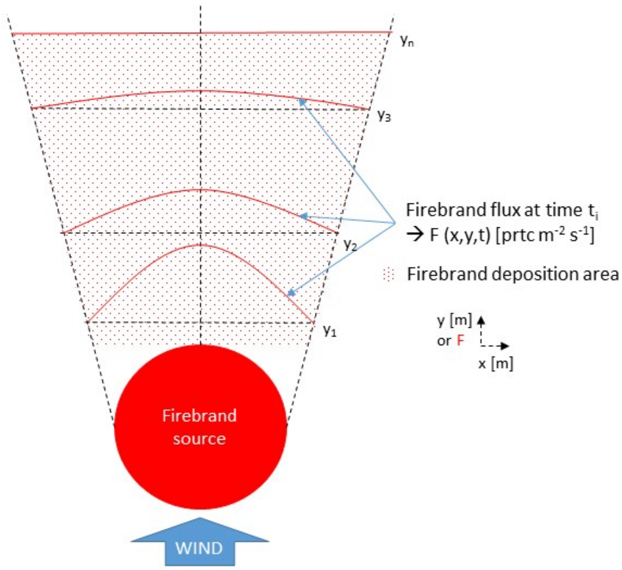

Figure 1 Schematic of the distribution of firebrand flux relative to the fire source.

The distribution of the collection sites is an important consideration. This requires evaluation of the likely fire conditions (including induced flows), fuels, and meteorological conditions. The collection site should be located in an arrangement that allows variations in firebrand flux to be evaluated as a function of distance from the fire line (the y coordinate in Figure 1) and perpendicular to the spread direction to be accounted for (the x coordinate in Figure 1). An additional consideration should be the density of collection sites as a function of the distance from the fire front. Close to the fire front, the number of firebrands has been shown to be higher and consequently a smaller number of collection sites (or cans) can be used. Further from the fire front, the flux of firebrands decreases so a larger number of collection sites should be used. Thomas et al. [20] showed that a collection area of diameter 4.5 m, did not result in significant variation of firebrand collection across the site area.

Plotting firebrand flux data as a function of separation from the burn unit (Figure 2) allows integration of a fitted curve to determine to total number or mass of firebrands. This can be compared with firebrand generation data. This methodology can be used to generate firebrand distributions as a function of fire behaviour, fuels, meteorological conditions etc. for use in practical risk assessment tools.

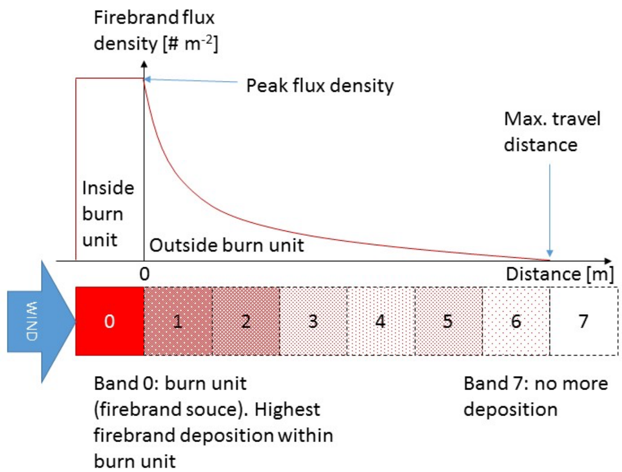

Figure 2 Schematic of firebrand deposition as a function of distance from the fire front

Real time firebrand flux and condition measurement

The firebrands collected using the technique described above represent the total firebrand exposure and do not provide any information about the thermal condition of the firebrands upon landing. Firebrand deposition is generally not constant throughout a fire, with periods of high deposition (firebrand showers) contrasted with periods of low deposition due to changes in fire behaviour and environmental conditions. To assess this temporal component, visual observation of the time when firebrands arrive at a given location is required. The temporal component allows firebrand deposition to be linked to fire behaviour.

Video analysis techniques (visual and infrared) can rapidly provide measurements of the particle geometry and thermal condition and the number of particles deposited at a location as a function of time and hence relative fire position and behaviour. These techniques allow for rapid data analysis and the generation of statistical data required.

Fire behaviour quantification

Firebrand generation is a strong function of fire behaviour and therefore this should be measured in conjunction with firebrand deposition or generation studies. The important characteristics are fire front location (to allow travel distance calculation) and heat release rate (fire intensity) as this will govern the convective flows, heating and flame height which in turn will govern the firebrand generation and transport processes. Given the variability of these parameters over relatively short distances, they were measured high temporal and spatial resolution within the experimental burn units [26,27]. This has been achieved through the measurements of fire front arrival time using an array of GPS equipped thermocouples with a grid size chosen to reflect the fire behaviour/

Firebrand travel distance

Knowing the arrival time of particles and occurrence of firebrand showers can further be used to estimate firebrand travel distances. This requires knowledge of the fire front position. Correlating the time of arrival of particles at a given collection site and fire front position will allow estimation of travel distance. A simple estimation can be made by measuring the separation between collection site and fire front position in direction of the ambient wind at the time of arrival of particles. This provides a lower bound of the travel distance as it does not account for the particle trajectory. Currently, no feasible experimental techniques exist to track firebrands from source to deposition; CFD models are a likely candidate to shed more light onto this mechanism.

Results and discussion

Four experimental field campaigns, resulting in six fires, were undertaken:

- 2016 NJ Pine Barrens. Firebrand and fire behaviour data collected from one fire.
- 2017 NJ Pine Barrens. Firebrands and fire behaviour data collected from two fire.
- 2017 Tall Timbers. Firebrands and fire behaviour data collected from one fire.
- 2019 NJ Pine Barrens. Firebrands and fire behaviour data collected from two fires.

In addition laboratory studies of firebrand ignition propensity were undertaken as well as implementation of a firebrand transport model in Fire Dynamics Simulator.

Data from the 2016 Fire is available in Thomas et al. [9]. Data from the 2017 fires is in preparation for journal submission. Data for 2019 in preparation for submission to a Journal. The firebrand ignition study is available in Thomas et al. [28]. This report will present the key results from each objective and will conclude with a discursive summary.

2016 NJ Pine Barrens (Objectives 1 and 2)
Full details of the experimental site, fuel characterisation and fire behaviour are given in Thomas et al. [9].

This work was undertaken in the Pineland National Reserve of NJ, USA in a pitch pine dominated ecosystem. The understory was characterised by various shrubs. The burn area was approximately 28 hectares and is shown in Fig. 1. The burn area was defined by existing access roads. Measurement site locations were selected on the criteria that the collection of firebrands occur outside of the parcel. The positioning of the sites was finalised based on the intended ignition pattern required to generated a head fire in the direction of the firebrand collection sites.

Fire behaviour measurement and firebrand collection

Local fire behaviour was evaluated based on flame height measurements recorded close to the collection sites. The fire line intensity was calculated using two measurements: flame height and fuel consumption (from destructive sampling). The location of fire behaviour packages (FBPs) are given in Figure 2.

Circular aluminium cans were used to collect firebrands. Cans were of 22 cm diameter and 12 cm height. Cans were filled with water to extinguish firebrands upon landing. Other extinguishing media was found to be less effective or to interfere with firebrand characterisation. Details of a Firebrand collection site (FCS) are shown in Figure 3. The temporal component to firebrand deposition was identified using video cameras located at each FCS. The relationship between the location of FCS and fire behaviour measurements are given in Table 1.

An initial aim was to assess the variability of firebrand collection within a FCS. Therefore three legs were used to assess the variation in firebrand collection relative to the firebrand arrival direction.

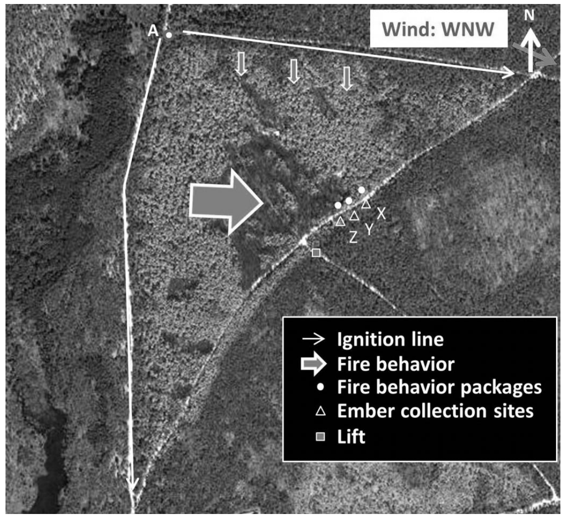

Fig. 1. Satellite image of burn unit (post fire). Indicating, general wind direction, ignition pattern, data collection package locations (FBP, FCS) and overall fire spread direction. The dark area corresponds to an area of high consumption of canopy fuel. Reproduced from Thomas et al. [9].

Table 1. Separation distances [m] between FBPs and FCSs.

	FBP Z	FBP Y	FBP X
FCS Z	27	29	60
FCS Y	29	21	32
FCS X	58	40	20

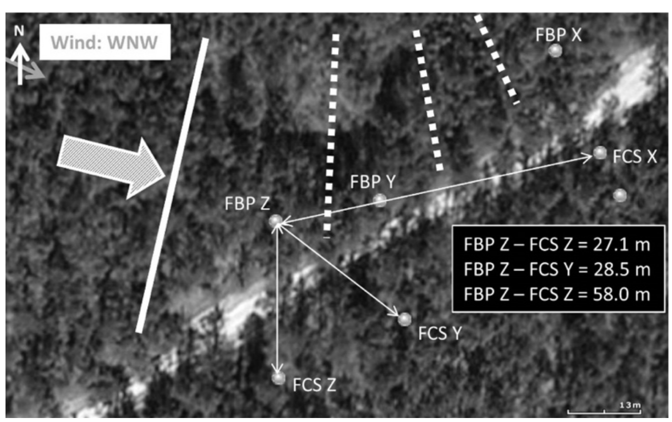

Fig. 2. Location of FBP and FCS with observed fire propagation (large arrow, solid and dotted lines). Reproduced from Thomas et al. [9].

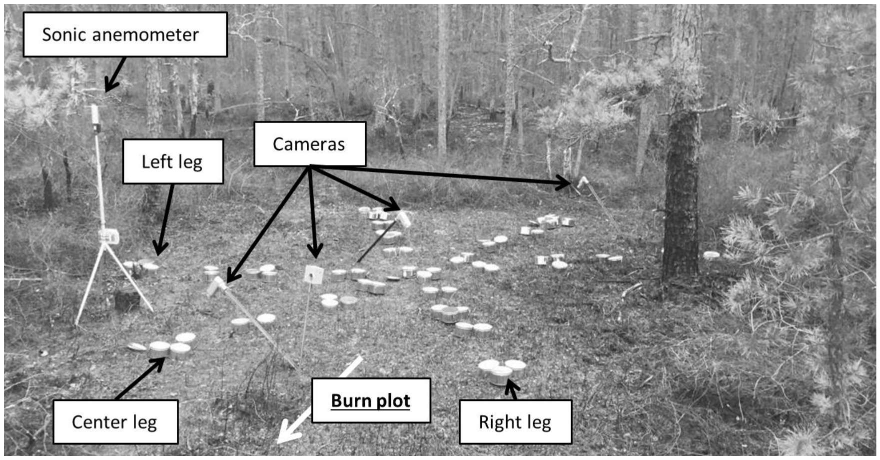

Figure 3 Photograph of a typical FCS. Reproduced from Thomas et al. [9].

Fire behaviour

The general fire behaviour was that the fireline impacted the measurement areas from a west-northwesterly direction (Figure 2). FBP Z was approached first. The northern ignition spread more slowly with less intensity due to the non-alignment with the wind.

Local fire behaviour is shown in Figure 4. Using correlations based on flame height, intensities of ~1.7 $MW.m^{-1}$ and 8.6 $MW.m^{-1}$ are calculated for FBP X and FBP Z, respectively. Using fuel consumption, higher estimates are made of 7.35 ± 3.48 $MW.m^{-1}$ and 12.59 ± 5.87 $MW.m^{-1}$ for FBP X and FBP Z, respectively. Independent of the measurement used, it is clear that the fire is of greater intensity at FBP Z than at FBP X.

Firebrand collection

The typical result of firebrands collected in a collection can are shown in Figure 5. Details of the image processing applied can be found in Thomas et al. [9]. Analysis showed that there was no significant difference in the firebrands collected within the area of a FCS. This analysis also allowed the total number of firebrands deposited at a site to be calculated using image processing techniques.

a) Fire a FBP Z b) Fire a FBP Y c) Fire a FBP X

Figure 4 Still shots from video footage observing the fire behavior at each FBP: (a) fire is at FBP Z, (b) at FBP Y, and (c) at X. The camera in (a) and (b) is located just in front of FCS Y. The camera in (c) in front of FCS X. The line indicates the location of the fire behavior package (FBP) in each site. Reproduced from Thomas et al. [9].

Figure 5 Standardized photograph of the inside of a typical aluminum firebrand collection can (diameter: 22 cm) with firebrands.

The second analysis step involved evaluating the arrival time of the firebrands in order to evaluate the firebrand flux and to relate this to the fire position. Table 2 shows data relating to the firebrand arrival and durations of high firebrand deposition ("firebrand showers").

Table 2. Results of video analysis: first and last particle arriving, duration of firebrand collection, and timing of firebrand showers. Times are from ignition.

	FCS Z	**FCS Y**	**FCS X**
1st firebrand arriving [mm:ss]	12:13	12:50	13:24
Firebrand showers [mm:ss]	16:38-18:40	17:53-19:00	18:05-19:37
Last firebrand arriving [mm:ss]	18:47	20:23	19:11
Duration of collection [s]	394	513	407

Using the data above, it is possible to calculate the firebrand flux (i.e. the number of firebrands arriving per unit area per unit time). These data are shown in Table 3.

Table 3. Firebrand collection analysis: firebrand density, duration of collection and total firebrand flux.

	FCS Z	**FCS Y**	**FCS X**
Firebrand density [$pcs.m^{-2}$]	536	463	335
Time span [s]	394	513	407
Total firebrand flux [$pcs.m^{-2}.s^{-1}$]	1.361	0.902	0.824

Summary

From these experiments, it was clear that:

- There is a significant temporal variation in the firebrand deposition process.
- Firebrand generation is strongly influenced by local fire behavior and fuel conditions.
- Higher spatial resolution of fire spread data is required.
- Larger separation distances of FCS would be desirable to capture a stronger spatial dependency.

- The value of collection cans is significantly enhanced if a temporal component can be added to the collection data.

2017 NJ Pine Barrens and Tall Timbers (Objectives 1 and 2)
Full Details of the experimental site, fuel characterisation and fire behaviour are given in Thomas et al. [29] (in preparation).

Two experiments were conducted at sites in the New Jersey Conservation Foundation Franklin Parker Preserve, within the New Jersey Pinelands National Reserve. The first unit was 13.8 ha and was burned during the evening of 6 March 2017, while the second unit, was 15.4 ha and was burned during the morning of 23 March 2017. These units will be referred to as PPS and PPN, respectively. Neither unit had burned or been managed since a major wildfire in the spring of 1954. The forest overstory in each unit was heavily dominated by pitch pine (*Pinus rigida* Mill.), and the understory was comprised of mixed ericaceous shrubs, shrub oaks, and associated species. Previous prescribed fires in this landscape are described by [9,10,27,30,31].

The third unit was located at the Tall Timbers Research Station & Land Conservancy in southern Georgia. This site covered an area of 2.4 ha and was burned on 21 April 2017. This site will be referred to as TT. Prior management of this stand included a prescribed fire approximately one year prior to the current study. The forest overstory in this stand was comprised of a monoculture of longleaf pine (*Pinus taeda*), while the understory was comprised primarily of sweet gum (*Liquidambar styraciflua*), wiregrass (*Aristida stricta*), various southern shrub form oaks (*Quercus. Spp.*), and other forbs typical of the longleaf–wiregrass ecosystem.

Fire behaviour measurement and firebrand collection

To obtain higher resolution fire behaviour data it is desirable to have information on fire front position function of time. From this data, spread rate and fire intensity can be derived. To obtain this, an array of 100 “fire trackers” (independent GPS enabled, single channel temperature measurement devices) were built. The spacing of fire trackers is shown in Figure 6. This is a novel contribution made possible by the funding secured from this project and associated leverage. In addition, nine 6.5 m tall understory towers were used to measure the vertical profile of gas temperature at the locations identified in Figure 6.

An additional set of firebrand measurements were made using a novel firebrand flux and condition system (FFCS) made possible through NIST grant *Development of a Firebrand Flux and Condition System* (Federal Funding ID: 70NANB16H280). Two FFCS were deployed in these fires. Analysis and interpretation of these results are available in Zen et al. [32] (in preparation).

Eight FCSs each with 15 water-filled cans, were used in each experiment. Cans were placed randomly within a 3 m^2 area. Measurement of the time-dependent the firebrand flux was made using a video camera facing into one can at each FCS.

Figure 6 highlights the arrangement of the FCSs in relation to the burn units. FCSs were arranged on two transects (left and right) with nominal 50 m separation distance between transects. Collection sites in each transect were separated by 25 m. FCS L1/R1 are closest to the burn unit, and L4/R4 are farthest away. This alignment was chosen according to the prevailing wind direction and to capture any change in firebrand deposition as a function of distance from the fire front. The number of firebrands and the size (projected area) were measured by processing an image of each can after the fire [9].

As previously, fire line intensity was calculated using fuel consumption and flame height methods.

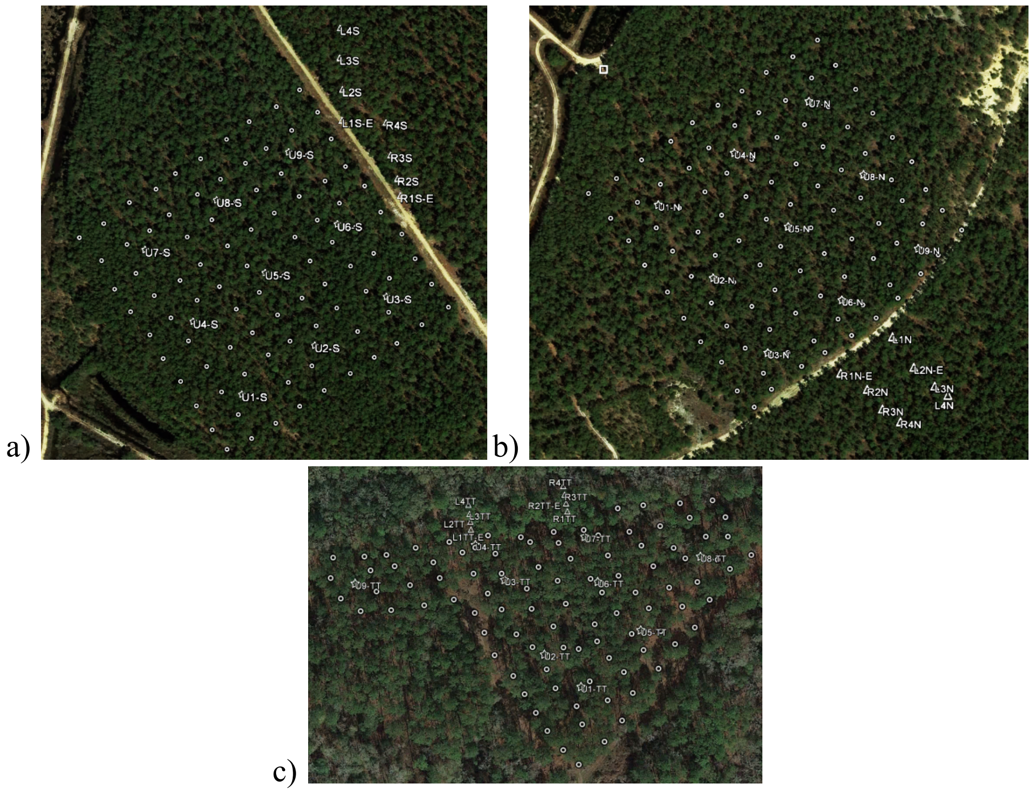

Figure 6 Site layout for 2017 experimental burns. (a) PPN, (b) PPS and (c) TT. Circles: Fire tracker, Stars: Understory towers, Squares: Overstory tower, Triangles: Firebrand Collection Sites.

Fire behaviour

Spread rate maps were for the three burns are shown in Figure 7. In no case did the fire spread as a continuous fire line in a single direction. This was the result of either complex ignition patterns (PPS and TT) or features such as spot fires and fuel discontinuity (PPN). Average spread rates are given in Table 4.

The PPN burn had the highest spread rate, with the highest local values of spread rate occurring between 7-9 minutes and 13-15 minutes after ignition. This was followed by the PPS burn, which, although having a lower overall spread rate, had moments of locally high spread rates between 40-46 minutes after ignition. The TT burn had a significantly lower spread rate than those in the Pitch Pine ecosystem, with a mean value which is nearly an order of magnitude below that of the PPN and PPS burns (Table 4). Further, there were no notable instances of locally high spread values in this experiment, with the TT burn having the lowest relative standard deviation in spread rate.

Comparing the tabulated values to previous work in similar fuels [9,33], the PPN burn falls in the range of a high intensity surface fire with local crown involvement, the PPS burn was a moderate to high intensity surface fire, and the TT burn was a low intensity surface fire.

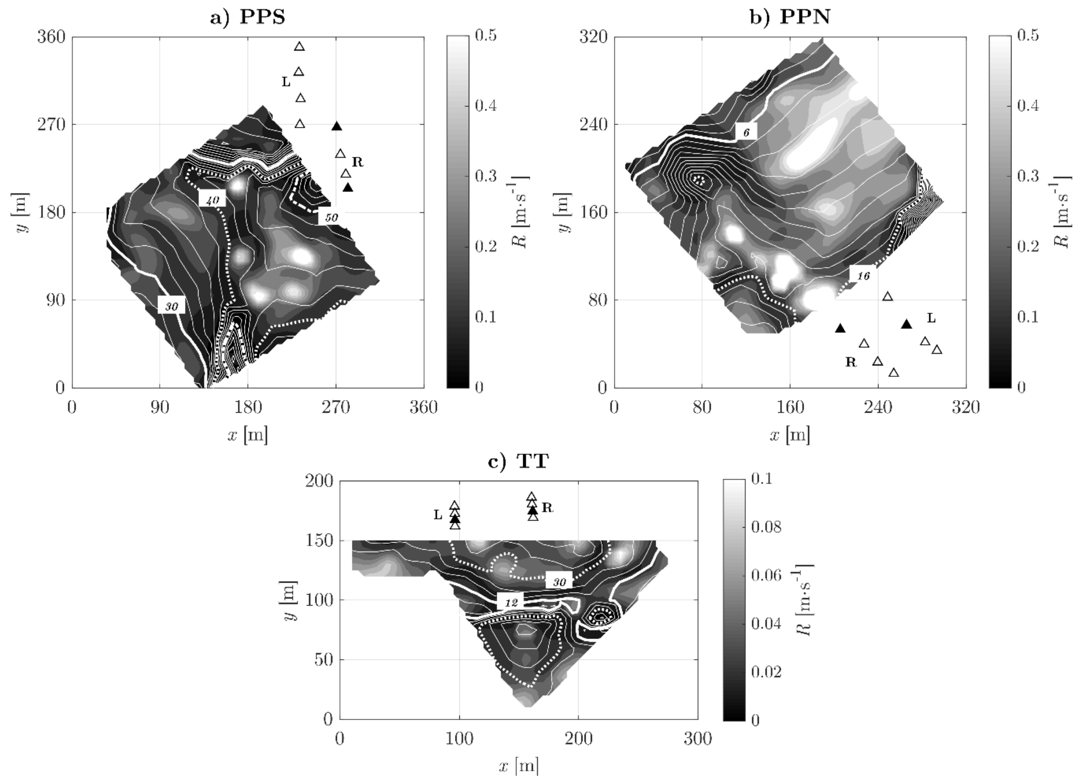

Figure 7 Spread rate maps for three experiments: (a) PPS, (b) PPN and (c) TT. Grayscale shading corresponds to spread rate. White contours are isochrones of fire position, shown in minutes from ignition for every (a) 2-min, (b) 1-min, and (c) 6-min. Specific isochrones are highlighted, with corresponding times labeled. Firebrand collection sites are shown as triangles, with black triangles indicating the location of sonic anemometers (3 m AGL).

Table 4. Plot average (±1 SD) spread rate and fireline intensity.

Burn	Rate of spread [m·s^{-1}]	Fireline intensity [kW·m^{-1}]	
		Fuel cons.	Flame length
TT	0.035 ± 0.017	700 ± 600	< 230
PPS	0.142 ± 0.093	4200 ± 3200	1420 ± 1786
PPN	0.257 ± 0.155	10800 ± 7000	7570 ± 5670
2016 (surface) [REF]	0.289 ± 0.014	7350 ± 3480	1700
2016 (torching) [REF]		12590 ± 5870	8600

Firebrand collection

It can be seen in Figure 8 that the flux density is significantly different for the three experiments, suggesting a relationship between fireline intensity and firebrand production. The highest flux density was during the PPN burn with each FCS recording higher flux densities than PPS. TT shows the lowest flux density, even with much shorter separation between the FCS and the burn unit. Comparing the global fire intensities for each burn (Table 4) there appears to be a relationship between fire intensity and firebrand flux. Differences between TT and PPN/PPS may also be due to fuel type (different ecosystems) however, the relationship between fire intensity and fuel type is not further explored here.

Results show variability between collection-transects within a single experiment (Figure 8). For example, the right transect in PPN (PPN-R) had a greater firebrand exposure compared to the left transect (PPN-L). In PPS, the left transect (PPS-L) had a greater exposure than the right transect (PPS-R). These local variations are likely driven by local wind and fire behaviour conditions. Furthermore, this might also explain the trends for PPS, where it appears that a combination of variation in local fire behaviour and wind conditions resulted in a less strong relationship.

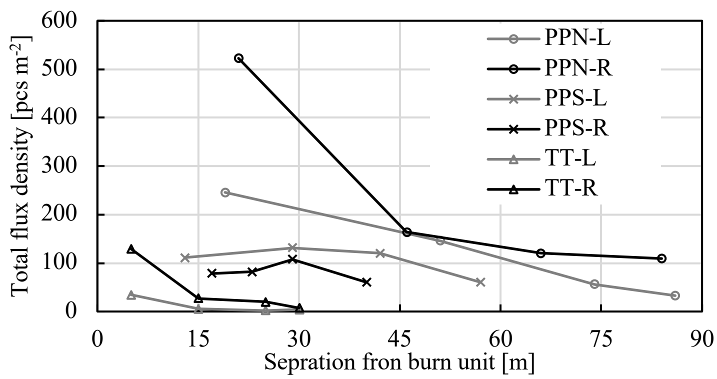

Figure 8 Total firebrand flux density as a function of separation distance for 2017 burns

Data for projected firebrand area from each experiment is shown in Figure 9(b) which includes data from 2016. Only small differences can be observed between PPN and PPS, most notably that the PPN fire produced larger particles. Comparing results from PPN and PPS to 2016 data shows that firebrands in 2016 were, on average, larger. The separation distance for collection sites to the burn unit in 2016 was in the same range as in 2017. The differences in particle characteristics are most likely due to fire behaviour and environmental conditions. Fire behaviour quantification discussed above showed that the 2016 experiment had the highest global spread rate and fire intensity (Table 4). Particles collected during the TT burn are significantly smaller than from the other experiments. This is a result of the low fire intensity for this burn, but also may be related to different fuel conditions.

The cumulative data in Figure 9 shows evidence of a relationship between fire intensity and characteristic size of firebrands: Low intensity surface fires produce only small particles, high intensity fires with crown involvement produce larger particles. This is an intuitive observation, however, the data set presented here is the first to provide quantification of this phenomenon.

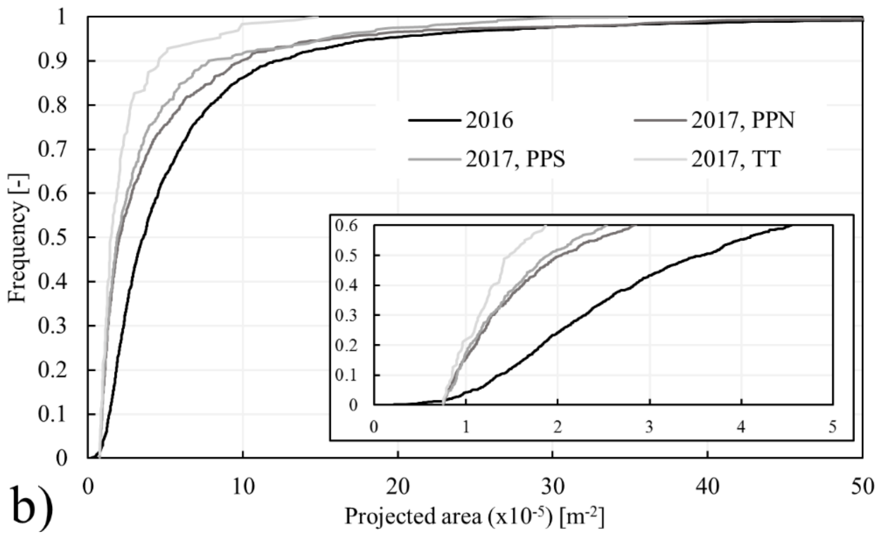

Figure 9 Firebrand characterization: Projected area represented in CDF. (a) right transect in PPN, (b) combined CDF for 2016, PPN, PPS and TT data.

The time dependent firebrand deposition at each FCS is given in Figure 10. This shows that the first particles landed 7 min after ignition. This occurred at L3 (i.e. not closest to the fire front). At this time the fir front is approximately 150 m away from the edge of the burn unit. Therefore the minimum distance travelled by this particle was 225 m (since trajectory and velocity are unknown). The last particle collected was deposited approximately 23 min after ignition.

Shaded areas indicate periods of rapid fire spread. It is possible that the periods of high intensity firebrand deposition are related to the periods of more intense fire behavior (inferred form rapid spread rate). Although it is not possible to be definitive in this statement (as the firebrand generation is not explicitly measured, the first period of high intensity spread could be responsible for the deposition between 10 and 13 min while the second period of high intensity spread could be responsible for the deposition between 14 and 17 min.

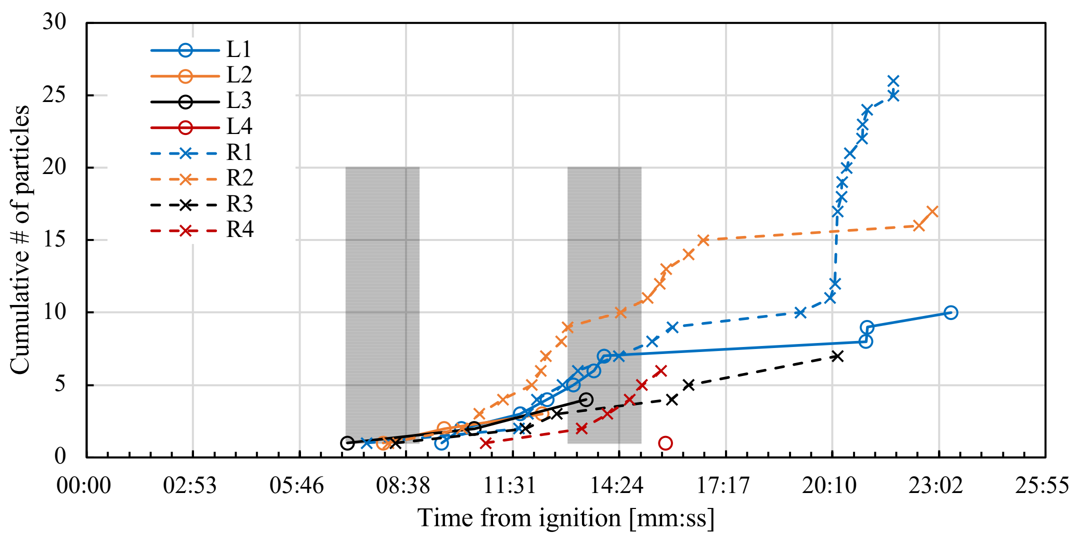

Figure 10 Time line of firebrand collection of the PPN experiment (single sample can per FCS).

Summary

- Deployment of fire trackers allowed continuous measurement of fire behaviour.
- Firebrand flux decreases as distance from the burn unit is increased.
- Cumulative distribution function allows comparison of firebrand projected area.
- Deployment of FFCS allows automatic characterisation of firebrands.
- Time dependent firebrand deposition behaviour can be related to fire behaviour.
- Lack of information of particle trajectory prohibits explicit relationship between fire behaviour and deposition being developed.
- A relationship between the firebrand deposition and the fire front has been proposed.

2019 NJ Pine Barrens (Objectives 1 and 2)
The final field campaign was undertaken in 2019 (after an extension due to inclement weather in 2018). The site was similar in fuel loading, structure to the 2017 NJ sites. The primary aim of this fire was to further develop the relationship between fire intensity and firebrand deposition distance identified in the 2017 fire.

Fire behaviour measurement and firebrand collection

To achieve this aim, the fire behaviour measurements remains the same however a greater number of firebrand collection sites were implemented to attempt to capture a greater degree of spatial variation in firebrand deposition (perpendicular to and parallel to the fire spread direction). The site layout is presented in Figure 11. Thirty firebrand collection sites were created each comprising 15 cans in an area of 3 m^2 (to allow comparison with data from 2017).

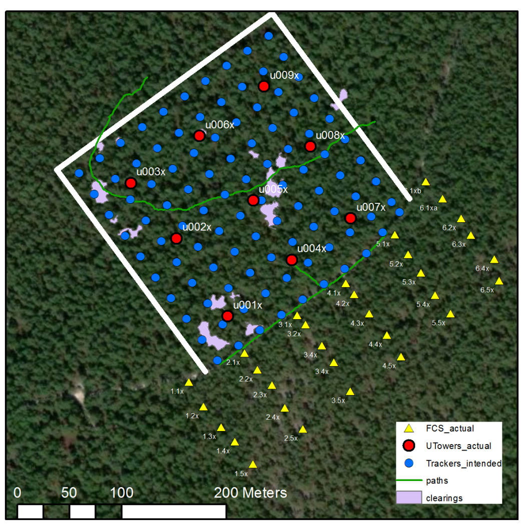

Figure 11 Site layout for 2019 experimental burns.

Fire behaviour

The rate of spread of the fire is shown in Figure 12. The rate was relatively low compared to the 2017 fire corresponding to low intensity (no data is presently available on the calculated values of fire intensity). However, two periods of high fire intensity were observed: between 30 and 40 mins in the eastern corner of the burn unit and between 56 and 64 min at the southern corner.

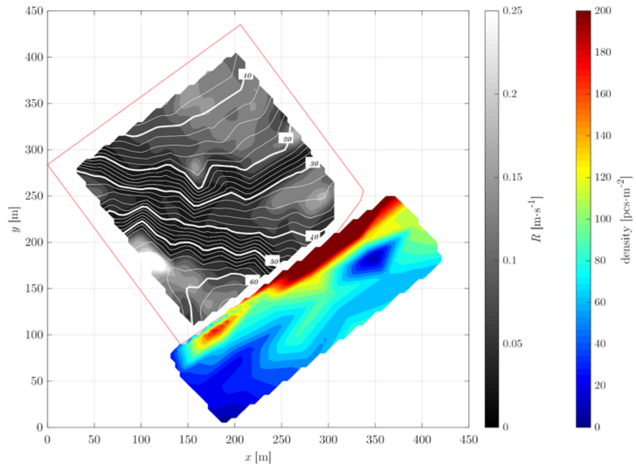

Figure 12 Fire spread (contours) and firebrand deposition (heat map) for the 2019 fire.

Firebrand collection

Firebrand deposition is at each of the collection sites is shown in Figure 13. The CDFs indicate that there firebrand characteristic are similar to those obtained previously. However the sites in which a significant number of firebrands was observed are restricted to those close to the burn unit (due to the low fire intensity). This is visualised in Figure 12. The highest firebrand flux density corresponds to the periods of rapid fire spread and high fire intensity in the eastern corner of the burn unit. The maximum firebrand deposition is a similar magnitude to that observed in the 2017 fires.

Summary

- Deployment of fire trackers allowed continuous measurement of fire behaviour.
- Firebrand flux measured as a function of distance from the fire line.
- Cumulative distribution function allows comparison of firebrand projected area.
- Deployment of FFCS allows automatic characterisation of firebrands.
- Time dependent firebrand deposition behaviour can be related to fire behaviour.

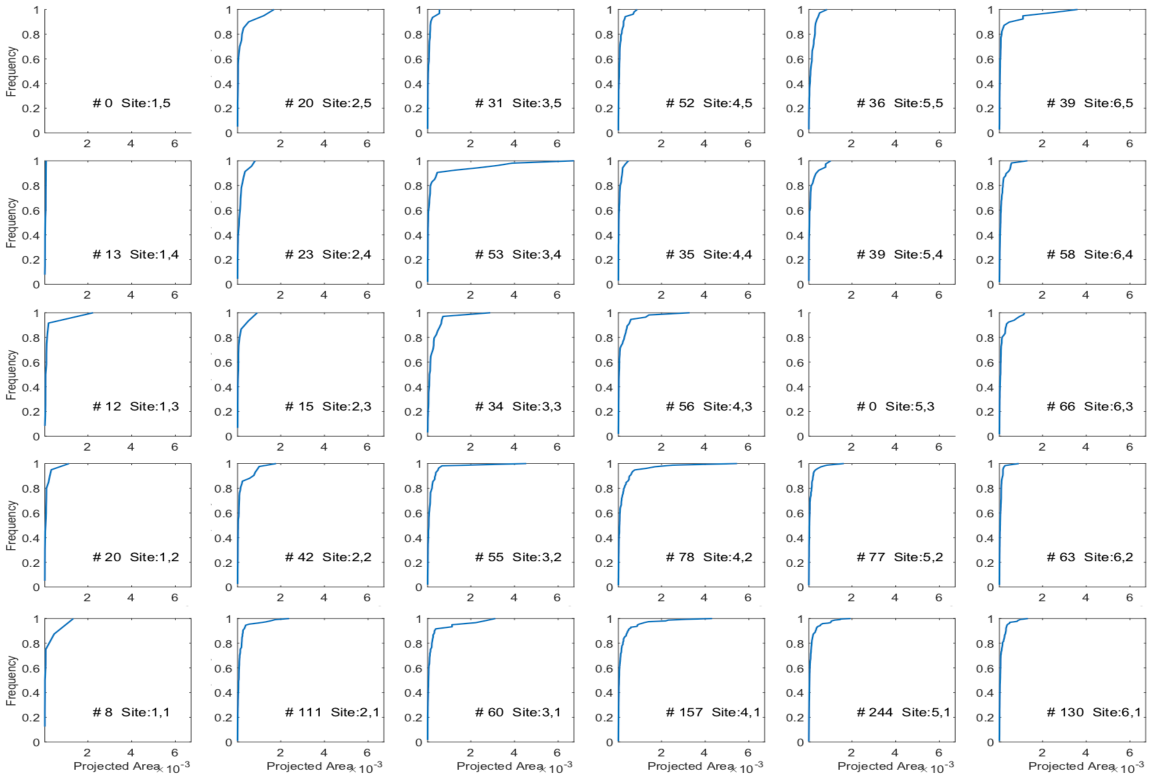

Figure 13 CDF of firebrand projected area collected at each collection site.

Firebrand ignition studies (Objective 3)

Full details of this objective are given in Thomas et al. [28]. The risk posed by firebrands was determined by evaluating the heat flux from accumulations of differing deposition area and mass. The experimental apparatus is shown in Figure 14 and the details of the instrumentation (used for the inverse heat transfer model) and the accumulation containment are shown in Figure 15.

Firebrands were conditioned using a muffle furnace for 10 minutes at the temperatures specified in Table 5. In general, increasing the degree of pyrolysis (i.e. higher temperatures) increased the heat of combustion of the firebrands. Note that since the primary mode of burning is smouldering, the direct application of heat of combustion may not be appropriate.

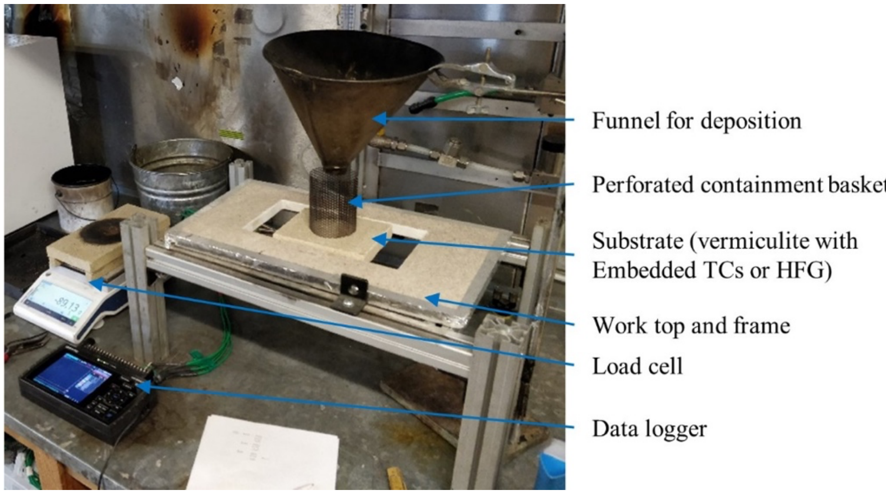

Figure 14. Experimental setup for generation of firebrands and measuring net heat flux from firebrand accumulations.

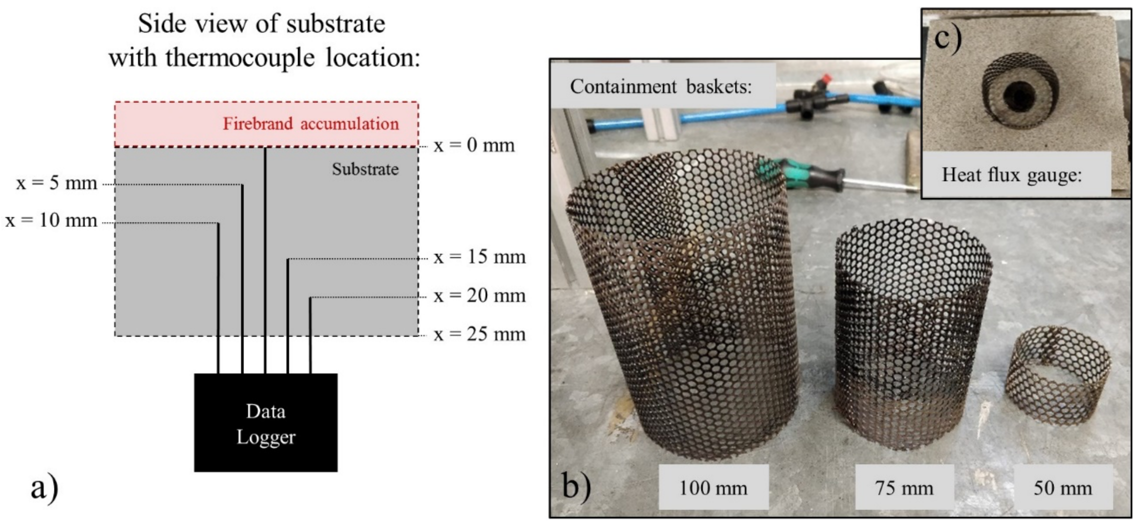

Figure 15. (a) Schematic of thermocouple layout and (b) containment baskets and (c) heat flux gauge in substrate (with 50 mm basket).

Table 5. Heat of combustion results from Bomb Calorimeter experiments (Three repetition per condition).

		Heat of comb. [kJ g^{-1}]	
Initial mass [g]	Furnace temp. [°C]	Avg.	St.dev.
-	-	18.78	0.06
-	-	19.92	0.03
200	400	21.86	2.14
100	400	22.61	2.34
50	400	28.81	0.04
100	600	33.54	0.03
50	800	32.39	0.06

The peak net heat flux i.e. the energy absorbed by the substrate is show in Figure 16 for different furnace temperatures and firebrand accumulation mases. The peak heat flux increases linearly as the degree of pyrolysis of the firebrand increases. There does not appear to be a strong relationship between heat flux and firebrand accumulation mass. The peak and average gauge and net heat flux for a subsample of conditions is given in Table 6. Both the gauge and net peak heat flux increases with oven temperature and decreases as the firebrand accumulation are increases for a constant mass.

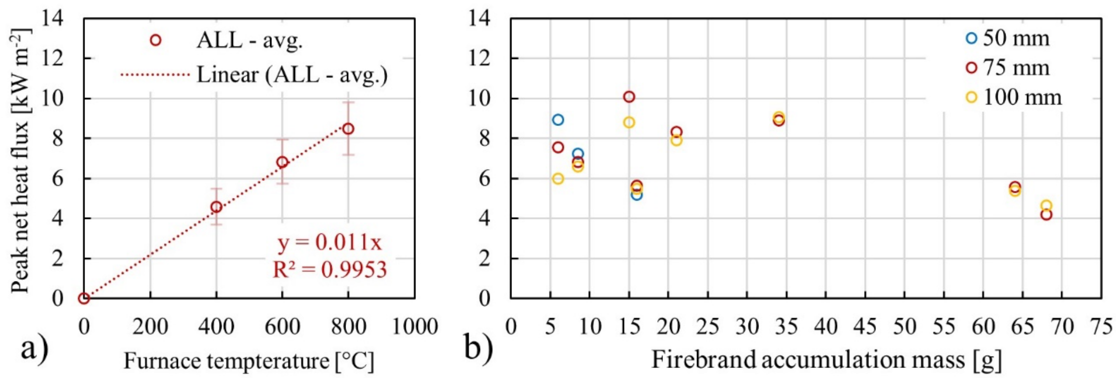

Figure 16. (a) Averaged Peak net heat flux vs furnace temperature. Error bars: one standard deviation. (b) Peak net heat flux plotted against accumulation mass.

Table 6. Summary of peak and 1-min averaged heat fluxes. The average is the first minute after deposition.

Initial mass [g]	Oven temperature [°C]	Accumulation diameter [mm]	Gauge heat flux [kW m^{-2}]		Net heat flux [kW m^{-2}]	
			Peak	1-min avg.	Peak	1-min avg.
50	400	50	39.6	17.4	5.63	3.11
50	400	75	35.3	13.7	5.47	2.76
50	400	100	30.9	15.2	5.20	2.52
50	800	50	79.8	21.5	8.93	5.06

The heating duration (Figure 17) is a strong function of the sample area and the accumulation mass. This is indicative that the smouldering of the firebrand accumulation controls the hazard.

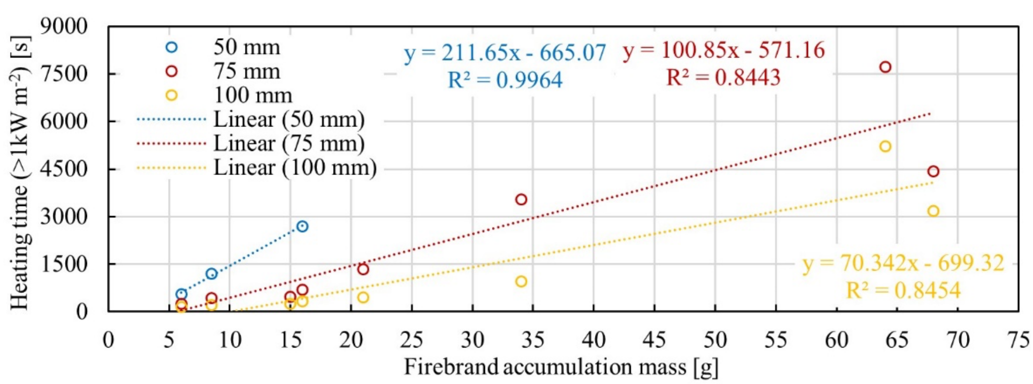

Figure 17. Duration for which the substrate is heat with at least a net heat flux > 1 kW m^{-2} plotted against firebrand mass (as deposited). The values in the legend refer to the deposition area diameter. The dotted lines are regression lines as indicated.

Summary

The heat fluxes produced by firebrand accumulations were measured using a water cooled heat flux gauge and by implementation of an inverse heat transfer model. The following conclusions can be drawn:

- The initial temperature of the particle on deposition is the primary driver of the peak heat flux to the substrate material.
- The duration of the exposure us a function of the mass of the firebrand accumulation and the deposition area; this is controlled by the smouldering of the accumulation.
- Smouldering of the accumulations may be sustained and is a function of the deposition area ,accumulation mass and particle properties.
- The absorbed heat fluxes are <10 kW/m^2 (net) and between 30-80 kW/m^2 (gauge)
- The heat flux from smouldering accumulations to the substrate was the range 5-7 kW/m^2 (net) and 1-3 kW/m^2 (net).

The findings show that high temperature firebrands many not represent most dangerous condition as these particles do not retain high temperatures for long periods of time. A prolonged exposure at lower heat fluxes (arising from lower temperature firebrands) may be sufficient to cause significant pyrolysis, degradation and charring of a substrate. These accumulations are capable of sustaining smouldering compared to fully charred particle accumulations. Thus, these may be considered more hazardous to solid combustible structural material.

Firebrand transport modelling studies (Objective 4)

A new method for adding firebrands to numerical simulations was proposed in the context of this project. Fire Dynamics Simulator (FDS) was used. Firebrands are generated in grid cells at surface level, for a given time step, based on the following:

$$n_f = \xi m_b'' \Delta x \Delta y \Delta t$$

Where is a conversion factor from mass of fuel consumed ($m_b'' \Delta x \Delta y \Delta t$) to number of firebrands generated - which, as of yet, is unknown and can only be found by tuning. The burning rate per unit area (m_b'') ensures that firebrands are only generated at the fireline, and allows the number to be scaled by the intensity of the fire. Any fractional firebrands are treated as a probability of creating an additional firebrand. This helps, in particular, to deal with the case of small grid cells and small time steps, where n_f might be less than one, but firebrands still have the potential to be generated.

An example output of firebrands generated from a stationary line fire, with an imposed wind, is shown in Figure 18. This case is using a fireline intensity (directly related to burning rate per unit area, m_b'') of 5 MW/m.

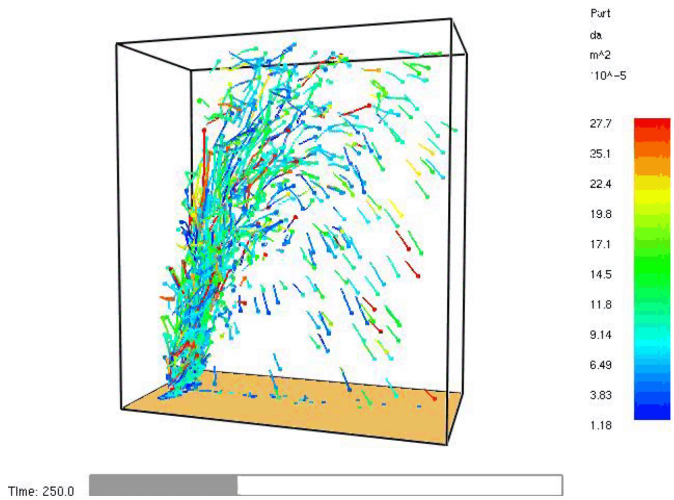

Figure 18 Firebrand generation from a stationary fire line with an imposed wind.

Firebrands in this figure are colored by their cross-sectional area. Particle area is randomly selected for each newly generated particle based on the inverse cumulative distribution function (i.e. inverse transform sampling method). This CDF was determined by extensive field measurement, as covered in other parts of this report, and takes the form of a modified exponential distribution:

$$F = 1 - 1.66e^{-1446x^{0.67}}$$

Where x is particle area in m^2.

From the numerical simulations of stationary line fires, run at a quasi-steady state for a given period of time, a map of the deposition pattern can be generated as shown in Figure 19. Comparison with real field data (Figure 12) suggests that this implementation qualitatively captures the deposition dynamics.

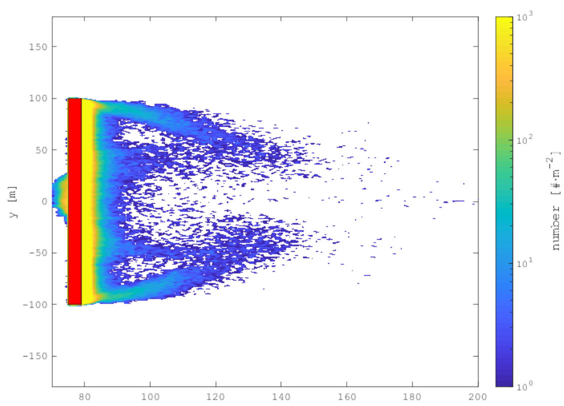

Figure 19 Map of firebrand deposition as a function of distance from the fire line

Eventually, these maps, when compared with experimental data on deposition patterns, can help to determine the magnitude and functional form of the coefficient . This will allow more complex simulations, with dynamic spreading fires, to be simulated with firebrand production, transport, and deposition included.

Conclusions

A methodology has been developed to simultaneously evaluate the time resolved firebrand flux and fire behaviour from field-scale fires. This has enabled the measurement of the number flux of firebrands and their projected area to be quantified. An initial assessment which shows that the number of firebrands generated can be related to fire behaviour however additional insight is required on the trajectory of the firebrands to identify an explicit relationship.

The key components of the methodology are:

- Time resoled fire dynamics – spread rate and fire intensity using a regular array of instrumentation.
- An array of firebrand collection sites to capture the total firebrand flux.
- Use of video analysis to determine the arrival of firebrands as a function of time.

These techniques are believed to be the minimum to establish realistic firebrand fluxes for use in risk assessment and implementation in predictive tools.

For the fire behaviours observed in the fieldwork, firebrand deposition was observed to have a strong dependency on distance from the fire front. Maximum firebrand fluxes of 500 pcs/m^2 were observed. Firebrand deposition was found to occur up to a distance of 200 m from the position of the fireline. Such trends were qualitatively reproduced in numerical modelling using FDS.

Firebrand ignition risk was found to be driven primarily by the initial temperature of the firebrands and the geometry of the accumulation. Peak gauge heat flues of 30-80 kW/m2 were measured corresponding to neat heat fluxes of 5-8 kW/m2.

This project has furthered the understanding of the risks associated to firebrand generation and deposition for fires of differing intensities and generated a unique set of experimental data from field experiments and quantified the risk through bespoke laboratory testing to generated data which identifies the nature of the risk posed by firebrands.

Future work

The following topics are proposed for further study:

- The relationship between firebrand generation and vegetation types and fire behaviours.
- The characteristics of firebrands during transport in the plume to improve the implementation of this in numerical modelling.
- Firebrand deposition characteristics resolved in space and time.
- Improved models of firebrand burning and cooling in transit for inclusion in computational codes.

References

[1] R. Hadden, S. Scott, C. Lautenberger, A. Fernandez-Pello, Ignition of Combustible Fuel Beds by Hot Particles: An Experimental and Theoretical Study, Fire Technol. 47 (2011) 341–355. doi:10.1007/s10694-010-0181-x.

[2] J.L. Urban, C.D. Zak, C. Fernandez-Pello, Cellulose spot fire ignition by hot metal particles, Proc. Combust. Inst. 35 (2015) 2707–2714. doi:10.1016/J.PROCI.2014.05.081.
[3] A.C. Fernandez-Pello, C. Lautenberger, D. Rich, C. Zak, J. Urban, R. Hadden, S. Scott, S. Fereres, Spot fire ignition of natural fuel beds by hot metal particles, embers, and sparks, Combust. Sci. Technol. 187 (2015). doi:10.1080/00102202.2014.973953.
[4] J.L. Urban, C.D. Zak, J. Song, C. Fernandez-Pello, Smoldering spot ignition of natural fuels by a hot metal particle, Proc. Combust. Inst. 36 (2017) 3211–3218. doi:10.1016/J.PROCI.2016.09.014.
[5] S. Santamaria, K. Kempná, J.C. Thomas, M. El Houssami, E. V. Mueller, D. Kasimov, A. Filkov, R. Gallagher, Michael, N. Skowronski, R.M. Hadden, A. Simeoni, INVESTIGATION OF STRUCTURAL WOOD IGNITION BY FIREBRAND ACCUMULATION, First Int. Conf. Struct. Saf. under Fire Blast CONFAB. (2015).
[6] S.L. Manzello, T.G. Cleary, J.R. Shields, J.C. Yang, Ignition of mulch and grasses by firebrands in wildland urban interface fires, Int. J. Wildl. Fire. 15 (2006) 427–431. doi:10.1071/WF06031.
[7] S.L. Manzello, T.G. Cleary, J.R. Shields, J.C. Yang, Ignition of Vegetation and Mulch by Firebrands in Wildland/Urban Interface (WUI) Fires, Chem. Phys. Process. Combust. (2006) 22. doi:10.1071/WF06031.
[8] S.L. Manzello, T.G. Cleary, J.R. Shields, J.C. Yang, On the ignition of fuel beds by firebrands, Fire Mater. 30 (2006) 77–87.
[9] J.C. Thomas, E. V. Mueller, S. Santamaria, M. Gallagher, M. El Houssami, A. Filkov, K. Clark, N. Skowronski, R.M. Hadden, W. Mell, A. Simeoni, Investigation of firebrand generation from an experimental fire: Development of a reliable data collection methodology, Fire Saf. J. 91 (2017) 864–871. doi:10.1016/j.firesaf.2017.04.002.
[10] M. El Houssami, E. Mueller, A. Filkov, J. Thomas, N. Skowronski, M. Gallagher, K. Clark, R. Kremens, A. Simeoni, Experimental Procedures Characterising Firebrand Generation in Wildland Fires, Fire Technol. (2015) 1–21. doi:10.1007/s10694-015-0492-z.
[11] A. Maranghides, D. McNamara, 2011 Wildland Urban Interface Amarillo Fires Report #2 - Assessment of Fire Behavior and WUI Measurement Science, (2011).
[12] A. Maranghides, W. Mell, A Case Study of a Community Affected by the Witch and Guejito Wildland Fires, Fire Technol. 47 (2011) 379–420. doi:10.1007/s10694-010-0164-y.
[13] N. Sardoy, J.-L. Consalvi, B. Porterie, A.C. Fernandez-Pello, Modeling transport and combustion of firebrands from burning trees, Combust. Flame. 150 (2007) 151–169. http://www.sciencedirect.com/science/article/B6V2B-4NWN3BN-2/2/125b9b8e2ba99cf7036f8c5d7e9df667.
[14] J.L. Urban, C.D. Zak, C. Fernandez-Pello, Spot Fire Ignition of Natural Fuels by Hot Aluminum Particles, Fire Technol. 54 (2018) 797–808. doi:10.1007/s10694-018-0712-4.
[15] G.C. Ramsey, N.A. McArthur, Building in the Urban Interface: Lessons from the January 1994 Sydney Bushfires, in: Bushfires 1995, Hobart, Tasmania, 1995.
[16] S.L. Manzello, T.G. Cleary, J.R. Shields, A. Maranghides, W. Mell, J.C. Yang, Experimental investigation of firebrands: Generation and ignition of fuel beds, Fire Saf. J. 43 (2008) 226–233. doi:10.1016/j.firesaf.2006.06.010.
[17] S.L. Manzello, T.G. Cleary, J.R. Shields, A. Maranghides, W. Mell, J.C. Yang, {E}xperimental investigation of firebrands: {G}eneration and ignition of fuel beds, Fire

Saf. J. 43 (2008) 226–233. doi:10.1016/j.firesaf.2006.06.010.
[18] S.E. Caton, R.S.P. Hakes, D.J. Gorham, A. Zhou, M.J. Gollner, Review of Pathways for Building Fire Spread in the Wildland Urban Interface Part I: Exposure Conditions, Fire Technol. 53 (2017) 429–473. doi:10.1007/s10694-016-0589-z.
[19] B.W. Barr, O.A. Ezekoye, Thermo-mechanical modeling of firebrand breakage on a fractal tree, Proc. Combust. Inst. 34 (2013) 2649–2656. doi:10.1016/J.PROCI.2012.07.066.
[20] J.C. Thomas, E.V. Mueller, S. Santamaria, M. Gallagher, M. El Houssami, A. Filkov, K. Clark, N. Skowronski, R.M. Hadden, W. Mell, A. Simeoni, Investigation of firebrand generation from an experimental fire: Development of a reliable data collection methodology, Fire Saf. J. 91 (2017). doi:10.1016/j.firesaf.2017.04.002.
[21] J. Hall, P.F. Ellis, G.J. Cary, G. Bishop, A.L. Sullivan, Long-distance spotting potential of bark strips of a ribbon gum (*Eucalyptus viminalis*), Int. J. Wildl. Fire. 24 (2015) 1109–1117. https://doi.org/10.1071/WF15031.
[22] J.P. Woycheese, Wooden disk combustion for spot fire spread, in: Interflam 2001, 2001: pp. 101–112.
[23] J.P. Woycheese, P.J. Pagni, D. Liepmann, Brand Propagation From Large-Scale Fires, J. Fire Prot. Eng. 10 (1999) 32–44. doi:10.1177/104239159901000203.
[24] E. Koo, P.J. Pagni, D.R. Weise, J.P. Woycheese, Firebrands and spotting ignition in large-scale fires, Int. J. Wildl. Fire. 19 (2010) 818. doi:10.1071/WF07119.
[25] C.S.S. Tarifa, P.P. del P. del Notario, F.G.G. Moreno, On the flight paths and lifetimes of burning particles of wood, Symp. Combust. 10 (1965) 1021–1037. doi:10.1016/S0082-0784(65)80244-2.
[26] E.V. Mueller, N. Skowronski, K. Clark, M. Gallagher, R. Kremens, J.C. Thomas, M. El Houssami, A. Filkov, R.M. Hadden, W. Mell, A. Simeoni, Utilization of remote sensing techniques for the quantification of fire behavior in two pine stands, Fire Saf. J. 91 (2017). doi:10.1016/j.firesaf.2017.03.076.
[27] E. V. Mueller, N. Skowronski, J.C. Thomas, K. Clark, M.R. Gallagher, R. Hadden, W. Mell, A. Simeoni, Local measurements of wildland fire dynamics in a field-scale experiment, Combust. Flame. 194 (2018) 452–463. doi:10.1016/J.COMBUSTFLAME.2018.05.028.
[28] J.C. Thomas, E. V. Mueller, R.M. Hadden, Estimating net heat flux from surrogate firebrand accumulations using an inverse heat transfer approach, Adv. For. Fire Res. 2018. 2017 (2018) 769–779. doi:10.14195/978-989-26-16-506_84.
[29] J.C. THOMAS, E. V. MUELLER, S. SANTAMARIA, M. GALLAGHER, K. CLARK, N. SKOWRONSKI, A. SIMEONI, R.M. HADDEN, Hazard assessment of short-range firebrand exposure, Int. J. Wildl. Fire. (n.d.).
[30] A. Simeoni, Z.C. Owens, E.W. Christiansen, A. Kemal, M. Gallagher, K.L. Clark, N. Skowronski, E. V. Mueller, J.-C. Thomas, S. Santamaria, R.M. Hadden, A preliminary study of wildland fire pattern indicator reliability following an experimental fire, J. Fire Sci. 35 (2017) 359–378. doi:10.1177/0734904117720674.
[31] A. Filkov, S. Prohanov, E. Mueller, D. Kasymov, P. Martynov, M.E. Houssami, J. Thomas, N. Skowronski, B. Butler, M. Gallagher, K. Clark, W. Mell, R. Kremens, R.M. Hadden, A. Simeoni, Investigation of firebrand production during prescribed fires conducted in a pine forest, Proc. Combust. Inst. 36 (2017). doi:10.1016/j.proci.2016.06.125.

[32] S. Zen, J.-C. Thomas, E. V. Mueller, B. Dhurandher, M. Gallagher, N. Skowronski, R.M. Hadden, Development of a field-scale firebrand flux and condition measurement system, (n.d.).
[33] E. V. Mueller, N. Skowronski, K. Clark, M. Gallagher, R. Kremens, J.C. Thomas, M. El Houssami, A. Filkov, R.M. Hadden, W. Mell, A. Simeoni, Utilization of remote sensing techniques for the quantification of fire behavior in two pine stands, Fire Saf. J. 91 (2017) 845–854. doi:10.1016/j.firesaf.2017.03.076.

Appendix A: Contact Information for Key Project Personnel

Dr Rory M. Hadden
School of Engineering
University of Edinburgh
Edinburgh, UK
r.hadden@ed.ac.uk

Dr Nicholas Skowronski
USDA Forest Service
Northern Research Station
Morgantown, VA
nicholas.s.skowronski@usda.gov

Dr Michael Gallagher
USDA Forest Service
Northern Research Station
Morgantown, VA
michael.r.gallagher@usda.gov

Dr Jan-Christian Thomas
School of Engineering
University of Edinburgh
Edinburgh, UK
c/o r.hadden@ed.ac.uk

Dr Eric V. Mueller
School of Engineering
University of Edinburgh
Edinburgh, UK
e.mueller@ed.ac.uk

Appendix B List of Completed/Planned Scientific/Technical Publications/Science Delivery Products

Journal Publications

1. J.C. Thomas, E.V. Mueller, S. Santamaria, M. Gallagher, M. El Houssami, A. Filkov, K. Clark, N. Skowronski, R.M. Hadden, W. Mell, A. Simeoni, Investigation of firebrand generation from an experimental fire: Development of a reliable data collection methodology, Fire Saf. J. 91 (2017). doi:10.1016/j.firesaf.2017.04.002.

2. A. Simeoni, Z.C. Owens, E.W. Christiansen, A. Kemal, M. Gallagher, K.L. Clark, N. Skowronski, E. V. Mueller, J.-C. Thomas, S. Santamaria, R.M. Hadden, A preliminary study of wildland fire pattern indicator reliability following an experimental fire, J. Fire Sci. 35 (2017) 359–378. doi:10.1177/0734904117720674.

Journal Publications in preparation

3. J.C. Thomas, E.V. Mueller, M. Gallagher, K. Clark, N. Skowronski, R.M. Hadden, Hazard assessment of short-range firebrand exposure.

4. S. Zen, J.-C. Thomas, E. V. Mueller, B. Dhurandher, M. Gallagher, N. Skowronski, R.M. Hadden, Development of a field-scale firebrand flux and condition measurement system.

Conference proceedings (peer reviewed)

5. J.C. Thomas, E. V. Mueller, R.M. Hadden, Estimating net heat flux from surrogate firebrand accumulations using an inverse heat transfer approach, Adv. For. Fire Res. 2018. 2017 (2018) 769–779. doi:10.14195/978-989-26-16-506_84.

Conference proceedings

6. Albert Simeoni, Zachary C. Owens, Erik W. Christiansen, Abid Kemal, Michael Gallagher, Kenneth L. Clark, Nicholas Skowronski, Eric V. Mueller, Jan C. Thomas, Simon Santamaria and Rory M. Hadden, A study of wildland fire direction indicator reliability following two experimental fires. International Symposium Fire Investigation, Scottsdale AZ, 2016.

Appendix C Metadata

Data types
The data recorded in this project are primarily comprised of two types: large scale and small-scale experimental data.

Large scale experimental data are:
- Measurements of temperature (stored as .csv)
- Video recordings inside and outside the burn units (.mp4)
- Infrared video recordings (.jpg, .mp4, .wmv and .seq (radiometric data))
- Firebrand size and geometry (.xlsx and .csv)

Small-scale experimental data are:
- Measurements of temperature (stored as .csv)
- Video recordings (.mp4)

Metadata
The following metadata are recorded for each experiment (small and large scale):

- experiment identifier
- date
- data type
- experiment conditions
- notes (observations)

These were recorded at the point of data collection and reviewed upon data storage.

Data management
The data will be managed according to the University of Edinburgh's Research Data Management policy (http://www.ed.ac.uk/information-services/about/policies-and-regulations/research-data-policy). Data shall be collected or converted and stored in non-proprietary formats (e.g. csv, jpeg) where possible. This is to allow ease of cross-platform use and long-term usability. Data sets will be assigned unique DOI numbers for long term preservation and sharing on the University of Edinburgh DataShare service (https://datashare.is.ed.ac.uk).